Published as: *Nat Cell Biol*. 2009 March ; 11(3): 247–256.

A Requirement of Nudel and Dynein for Assembly of the Lamin B Spindle Matrix

Li Ma[1,2], **Ming-Ying Tsai**[2,4], **Shusheng Wang**[2], **Bingwen Lu**[3], **Rong Chen**[2], **John R. Yates III**[3], **Xueliang Zhu**[1,*], and **Yixian Zheng**[1,2,*]

[1]Laboratory of Molecular Cell Biology and Center of Cell Signaling, Institute of Biochemistry and Cell Biology, Shanghai Institutes for Biological Sciences, Chinese Academy of Sciences, Shanghai, China

[2]Department of Embryology, Carnegie Institution for Science and Howard Hughes Medical Institute, Baltimore, Maryland, United States of America

[3]Department of Cell Biology, The Scripps Research Institute, La Jolla, California, United States of America

[4]Eppley Institute for Research in Cancer and Allied Diseases, University of Nebraska Medical Center, Omaha, Nebraska, United States of America.

Abstract

Guanosine triphosphatase Ran (RanGTP) can stimulate assembly of the type V intermediate filament protein, lamin B, into a membranous lamin B spindle matrix, which is required for proper microtubule organization during spindle assembly. Microtubules in turn enhance assembly of the matrix. We report here that the isolated matrix contains known spindle assembly factors such as dynein and Nudel. Using spindle assembly assays in *Xenopus* egg extracts, we show that Nudel regulates microtubule organization during spindle assembly independent of its function at kinetochores. Importantly, Nudel directly interacts with lamin B to facilitate the accumulation and assembly of lamin B-containing matrix on microtubules in a dynein-dependent manner. Perturbing either Nudel or dynein inhibited assembly of lamin B matrix. However, depleting lamin B still allowed formation of matrices containing dynein and Nudel. Therefore, dynein and Nudel regulate assembly of the lamin B matrix. Interestingly, we found that whereas depleting lamin B resulted in disorganized spindle and spindle poles, disrupting the function of Nudel or dynein caused a complete lack of spindle pole focusing. We suggest that Nudel regulates microtubule organization in part by facilitating assembly of the lamin B spindle matrix in a dynein-dependent manner.

Keywords

lamin B spindle matrix; Nudel; dynein; mitosis; cell fate determinants; membrane partitioning

*Correspondence: Yixian Zheng (zheng@ciwemb.edu) and Xueliang Zhu (xlzhu@sibs.ac.cn).

Introduction

NudE and Nudel (NudE-like) interact with dynein and regulate a diverse array of cellular functions, such as axonal transport and membrane trafficking 1,2,3, that require dynein. In addition, dynein has a number of mitotic functions, including spindle pole organization, spindle checkpoint control, and spindle orientation. Recent studies have shown that NudE and Nudel are involved in dynein recruitment to kinetochores in mitosis to regulate chromosome alignment and spindle checkpoint 4, 5. Overexpression of the N-terminus of NudE disrupts spindle assembly in mammalian cells 5, suggesting that like dynein, NudE and Nudel also participate in spindle organization. However, whether NudE or Nudel directly regulates microtubule (MT) organization independent of their roles at the kinetochore is unclear.

Lamins are type V intermediate filament proteins that form the nuclear lamina in interphase. They are important for nuclear functions including nuclear envelope assembly, DNA replication, and gene expression 6. Whereas the lamin A and C are found primarily in differentiated cells and are not required for cell viability, the ubiquitously expressed lamin B is essential for cell survival. Interestingly, RNAi-mediated reduction of lamin B in *Caenorhabditis elegans* 7 and HeLa cells 8 resulted in spindle defects, chromosome mis-segregation, and prometaphase delay. However, these studies could not distinguish whether lamin B has a direct role in spindle assembly or an indirect one due to failure in regulating interphase nuclear functions.

Using cytostatic factor (CSF)-arrested *Xenopus* egg extracts, we have demonstrated a mitosis-specific function of lamin B because depleting lamin B3 (LB3), the major form of lamin B in *Xenopus* eggs, causes defects in spindle assembly which can be rescued by bacterially expressed and purified LB3 protein 8. The spindle-associated LB3 exists in a membranous, matrix-like network whose assembly requires RanGTP and is enhanced by MT assembly. Since LB3 mutants known to disrupt nuclear lamina assembly also disrupt mitotic spindle assembly, LB3 appears to facilitate MT organization in the spindle as one of the structural components of the spindle matrix 8, 9.

Dynein and Nudel are known to mediate the transport, assembly, and organization of the cytoplasmic intermediate filament proteins such as vimentins 10 and neurofilaments (NF) 2. In fact, Nudel directly interacts with the light chain of NF (NF-L). After nuclear envelope breakdown during mitosis, dynein can mediate the transport of lamin-containing nuclear membrane remnants along the MTs 11, 12. Since all intermediate filament proteins share conserved structural features, we set out to examine whether Nudel and dynein could facilitate the assembly of the lamin B spindle matrix in a MT-dependent manner during spindle morphogenesis.

Results

Nudel directly interacts with lamin B

We found that epitope tagged human lamin B1 and Nudel reciprocally immunoprecipitated each other from HEK293T cells in the presence of detergent NP-40 (Fig. S1). Rabbit

polyclonal antibodies that recognized *Xenopus* Nudel, which shares ~80% amino acid identity with human and mouse Nudel (Fig. 1a; Fig. S2), could immunoprecipitate LB3 in egg extracts 8, 13 in the presence of detergent (Fig. 1b). LB3 antibodies immunoprecipitated dynein in a detergent-insensitive manner as judged by antibodies to dynein intermediate light chains 70.1 (Fig. 1c) or 74.1 (data not shown). It was, however, difficult to detect Nudel because it migrated just below the antibody heavy chain. Since similar immunoprecipitation results were obtained in the presence of nocodazole where neither LB3 nor Nudel antibody pulled down tubulin (Fig. 1d), LB3, Nudel, and dynein appear to interact with one another independent of tubulin or MTs.

Using purified 6His-tagged full-length Nudel (6His-Nudel, 1–345 aa), N- (6His-N-Nudel, 1–201 aa) and C-terminus (6His-C-Nudel, 167–345 aa) of Nudel (Fig. 1e; Fig. S3), we found that GST-tagged full length LB3 pulled down 6His-Nudel (Fig. 1f). All intermediate filament proteins contain a central α-helical-rod domain flanked by non-α-helical N- and C-terminal regions of variable lengths. The rod domain consists of two coiled-coil regions, coil1 and coil2. The coil2 is conserved among all intermediate filaments 14. We found that Nudel exhibited stronger interaction with GST-LB3-rod than GST-LB3T (Fig. 1g; Fig. S3). The coil2 region of LB3-rod appeared to mediate the interaction with Nudel (Fig. 1h). The C-terminus of Nudel mediated the interaction with the conserved coil2 of LB3 (Fig. 1i; j). Biosensor binding studies revealed that the equilibrium dissociation constant between Nudel and the coil2 domain of LB3 is ~50 μM (see Supplementary Information).

Nudel and dynein are components of the mitotic lamin B spindle matrix

To examine whether Nudel and dynein are components of the lamin B spindle matrix, we isolated the matrix using Aurora A (AurA)-bead based assay15 and subjected the matrix to protein sequencing. LB3 and a number of spindle assembly factors (SAF) including dynein were identified in the matrix but not Nudel (Supplementary Information, Fig. S4 and Table S1). Since proteomic analyses are not quantitative and may miss or falsely identify proteins, we also analyzed the isolated matrix using immunoblotting to assess the relative retention of dynein and Nudel on the matrix as compared to tubulin, TPX2, and LB3. Consistent with our earlier findings 8, the isolated matrix was completely disassembled in the presence of detergent (Triton X100). The matrix failed to assemble in the absence of RanGTP even when there was robust MT assembly as stimulated by DMSO. Both dynein and Nudel were present on the isolated matrix and they exhibited similar retention as LB3, whereas the vast majority of tubulin and TPX2 were not retained (Fig. 2a). Immunofluorescence analyses revealed that both dynein and Nudel exhibited similar distributions on spindles and spindle matrices to LB3 (Fig. 2b–e). Therefore, both dynein and Nudel are components of the lamin B spindle matrix.

Nudel regulates spindle assembly independent of its role at kinetochores

Previous studies of Nudel in mitosis have focused on its kinetochore functions 4, 5, 16. We used the AurA-bead assay, which does not involve chromosomes 15, to test whether Nudel regulates spindle assembly independent of kinetochores. Typically, AurA-beads began to nucleate MT asters between 1'–3'. These early asters had long MT arrays with no obvious bright MT core surrounding the beads (Fig. 3a, early aster). The early asters were

transformed into late asters between 3'–9' with increasing MT intensity (Fig. 3a, compare arrowheads in the early and late asters) and a clear bright MT core appearing around the AurA-beads (Fig. 3a, white dashed circle outlines the bright MT core). Then, the astral array of MTs began to shrink between 6'–11', which was accompanied by the expansion of the bright MT core surrounding the AurA-beads, resulting in the formation of a ball-like MT structure (Fig. 3a and b, MT balls are outlined by the white dashed circles in a). Using the ratio between the length of longest astral MT arrays attached to the MT core and the diameter of the bright MT core, we defined that a later aster has a ratio equal or greater than one, whereas a ball-like MT structure has a ratio less than one. Between 13'–15', most structures are MT balls or spindles and the ratio between the two structures varied, depending on the quality of egg extracts, from 9:1 (poor egg extracts) to 1:1 (good egg extracts) (Fig. 3a, b). For a given egg extract, the number of MT balls and spindles remained similar at 13' and 15'. Reaction times beyond 15' often resulted in aggregation of MT structures. Therefore, we focused our analyses up to 15'.

Since overexpressing the N-terminus of NudE in tissue culture cells disrupted mitosis 5, 17, we carried out the AurA-bead assay in the presence of excess GST-N-Nudel and found that both MT ball and spindle assembly were inhibited (Fig. 3c, d). In control reactions with GST addition, MT balls or spindles were assembled around AurA-beads by 13'–15' (Fig. 3d; Fig. S5). However, in the presence of GST-N-Nudel, most AurA-beads had late asters with long astral arrays of MTs (yellow arrowheads in Fig. 3d) attached to disorganized MT cores (yellow arrow in Fig. 3d). Similar to the addition of GST-N-Nudel, depletion of >95% of Nudel resulted in a severe block of assembly of MT balls and spindles, whereas adding back the purified 6His-Nudel fully reversed the defects (Fig. 3e). We found that *Xenopus* Nudel and NudE share 48% overall amino acid identity with each other and they appear to function redundantly in spindle assembly (Supplementary Information; Fig. 3e and Fig. S6a–c) independent of their roles in kinetochores 4,5,16,18.

Nudel and dynein regulate lamin B assembly on MTs during spindle morphogenesis

We examined whether Nudel and dynein might mediate the MT-dependent assembly of lamin B spindle matrix 8. Indeed, LB3 was localized along the astral MT arrays of the early AurA-asters (Fig. 4a). A network of LB3 surrounded the MTs by the late aster stage (Fig. 4a, yellow arrows on the late aster). As astral arrays of MTs shrank, LB3 was enriched on MT structures similar to γ-tubulin (Fig. 4a). Depletion of Nudel not only blocked assembly of MT balls and spindles as expected but also reduced the intensity of the LB3 network surrounding the late asters (Fig. 4b, compare the yellow arrows on the late asters in a and b). Addition of purified 6His-Nudel rescued the transition of late asters into MT balls and spindles (Fig. 4c) as well as the LB3 network surrounding MTs (Fig. S7). Dynein inhibition by 70.1 antibody produced similar results to Nudel depletion (Fig. 4c and Supplementary Information).

Next, we examined the effect of Nudel on LB3 assembly during spindle morphogenesis induced by demembranated *Xenopus* sperm. *Xenopus* sperm stimulated a consistent transformation of astral MT arrays into bipolar spindles. In the first 5'–10' of reactions, the MT asters induced by sperm had bright MT cores attached to radial array of MTs (Fig. 5a),

which began to polarize toward the sperm chromatin from 10'–20', and by ~30' most MT asters became half spindles (Fig. 5a). By 45'–120', depending on the quality of the egg extracts, 40–80% of sperm chromatin was associated with bipolar spindles (Fig. 5a).

The *Xenopus* sperm contained both Nudel and LB3 (Fig. 5b, c), which may partially compensate for the effect of Nudel depletion from the egg extracts. We found that depleting Nudel did not affect the assembly of MT asters in the first 5' (data not shown). The asters, however, became disorganized between 5'–15' (Fig. 5d). By 20', while the control asters accumulated LB3 network throughout the MT arrays, asters assembled in the absence of Nudel had a diminished LB3 network along the MT arrays (compare white and yellow arrowheads in Fig. 5e). Although the MT arrays were able to polarize toward the sperm between 20'–30', they were not focused at their minus ends (compare white and yellow arrows in Fig. 5e). By 45'–120', these structures further developed into fence-like parallel MT arrays around the chromatin (unfocused spindles) with diminished LB3 network on the MTs as compared to control spindles (Fig. 5f, compare white and yellow arrows and arrowheads). Both defects of MT organization and diminished accumulation of LB3 could be fully rescued by the purified Nudel (Fig. 5d–f).

Using the AurA-bead assay, we found that depleting Nudel caused a significant reduction of LB3 on MT structures in a time window between 6'–11' when the late asters transformed into MT balls and spindles. This reduction could be rescued by Nudel add-back (Fig. S7). Therefore, Nudel could facilitate the assembly of LB3 into spindle matrix by transiently concentrating LB3 on MTs.

Nudel and dynein regulate MT organization and lamin B matrix assembly

To assess the role of Nudel and dynein in lamin B matrix assembly, we prepared the matrix in the presence or absence of Nudel. Whereas depleting Nudel inhibited assembly of matrices containing LB3, addition of purified Nudel largely rescued the defects (graph in Fig. 6a). Any matrices formed in Nudel-depleted egg extracts were small as compared to controls, and many AurA-beads were not associated with any matrices (images in Fig. 6a). A similar lack of LB3-matrix assembly was seen when dynein was inhibited by 70.1 antibody (data not shown). We have shown previously that depleting LB3 prevented association of Eg5 with the spindle matrix, but depleting Eg5 or XMAP215 still allowed assembly of matrices containing LB3 8. Consistent with this, we found that inhibiting Eg5 using Monastrol 19 did not affect the assembly of matrices containing LB3, Nudel, or dynein (data not shown). Importantly, depleting LB3 still resulted in assembly of matrices containing Nudel and dynein (Fig. 6b). Like dynein 11, Nudel is localized to the nuclear envelope during prophase in tissue culture cells (Fig. S8). Therefore, Nudel and dynein are in the close proximity of lamin B at the onset of mitosis, which may facilitate their interaction with lamin B after nuclear envelope breakdown to regulate assembly of the lamin B spindle matrix.

We reasoned that Nudel and dynein could regulate spindle assembly in part by stimulating assembly of lamin B into the spindle matrix. Lamin B in the spindle matrix might in turn help MT organization. If this were the case, one might expect that depleting LB3 would result in MT disorganization in spindles, but the phenotype would be less severe as

compared to disrupting either Nudel or dynein. Using AurA-bead assay, we found that unlike disrupting the function of Nudel or dynein, which blocked both MT ball formation and spindle assembly (Fig. 4), depleting LB3 still allowed formation of MT balls and bipolar spindles (Fig. 6c). However, these MT structures were more disorganized than controls. Moreover, the MT balls formed in the absence of LB3 had a bigger diameter than those formed in control reactions (Fig. 6d). The bipolar spindles assembled in the absence of LB3 were also more elongated than those in controls (Fig. 6e).

Next, we analyzed the effect of LB3 depletion on MT organization during spindle morphogenesis stimulated by sperm chromatin. Similar to our earlier observation, depleting LB3 caused a reduction of normal spindle assembly. The majority of defective MT structures were multipolar spindles, half spindles, or asters (Fig. 7). As compared to Nudel depletion (see Fig. 5), removing LB3 from the egg extracts caused less severe defects in minus-end MT focusing. Assembly of MT asters appeared normal in the absence of LB3 before 15’ (Fig. 7a), whereas MT asters became highly disorganized after 5’ when Nudel was depleted (Fig. 5d). After 15’ in the absence of LB3, MT structures became disorganized with less MTs polarizing toward the sperm chromatin than that of mock-depletion (compare white and yellow arrows and arrowheads in Fig. 7b). However, comparing to Nudel depletion at the same time point, the polarized MTs were less splayed at the minus ends (compare Fig. 7b to Fig. 5e). Although depletion of LB3 disrupted spindle assembly (Fig. 7c), instead of having completely unfocused spindle poles as seen in Nudel depletion (Fig. 5f), defective spindles formed in the absence of LB3 had partially focused but often multiple poles (Fig. 7c).

Quantitative Western blotting revealed that 95–99% of LB3 was depleted in above experiments. Since LB3 is a structural protein, not an enzyme, the remaining 2–10 nM LB3 (LB3 concentration in egg extracts is ~200 nM) is most likely insufficient to perform a structural role. Indeed, similar spindle assembly defects occurred when less than 95% of LB3 was depleted in both the sperm and the AurA-bead-based assays (Fig. S9a–e). Thus, defective structures formed after LB3 depletion is not due to partial loss of LB3.

Discussion

Our studies suggest that Nudel and dynein function upstream of LB3 to promote assembly of LB3-containing spindle matrix in a MT-dependent manner. We show that Nudel is required for transiently concentrating LB3 onto MTs, probably through dynein-mediated transport of LB3 toward the minus ends of MTs. This could promote both LB3 self-association and association of LB3 with other components of the spindle matrix. Very little is known about the polymerization state of lamin and its mechanism of regulation in the interphase nuclear lamina or in the mitotic spindle. The finding that Nudel interacts with lamin B should help to further study the mechanism of lamin B assembly in mitosis.

Both Nudel and dynein have been found to participate in the organization of vimentin 10 and neurofilaments 2 in the interphase cytoplasm of tissue culture cells and in neurons, respectively. In neurons, Nudel interacts directly with NF-L. Here, we show that Nudel interacts with yet another intermediate filament, lamin B. Importantly, we demonstrate that

Nudel directly interacts with the region of lamin B that is conserved among all intermediate filament proteins. By interacting with both the intermediate filaments and MTs, Nudel and dynein may have a general role in coordinating the functions of the two cytoskeletal structures in animal cells.

Dynein functions in spindle pole focusing in animal cells 18, 20, 21. Our findings suggest that the dynein pathway regulates spindle pole organization, in part, by facilitating the assembly of lamin B into the spindle matrix in a MT dependent manner. Dynein is also known to facilitate the transport of NuMA to minus ends of MTs where NuMA helps to focus the minus ends into spindle poles 21. We have shown previously that NuMA localizes to the lamin-containing spindle matrix 8. Therefore, the dynein pathway may regulate spindle matrix assembly by targeting multiple components of the matrix, including lamin B and NuMA, to orchestrate spindle organization.

Nudel and dynein also have a well-established role in regulating membrane trafficking along MTs. Since we have shown that lamin B spindle matrix contains membranes and is disrupted by detergent, it is tempting to speculate that Nudel and dynein may use MTs to concentrate and incorporate multiple spindle matrix components, including lamin B, NuMA, and certain membrane compartments, into a functional spindle matrix. Such type of matrix may not only help MTs to regulate chromosome segregation but also use MTs to regulate the partitioning of cell fate determinants and membrane systems during cell division. Consistent with this, membrane-associated enzymes have been shown to regulate spindle morphogenesis 9, 22–24. Moreover, our mass-spectrometry analyses of the isolated lamin B spindle matrix have identified both SAFs and proteins with known functions in membrane trafficking and in cell fate determination (Table S1).

Conceptually, it is interesting to consider that the spindle matrix might organize the cell during mitosis in a similar manner as the interphase nucleus (Fig. S10). The interphase nuclear lamina helps to organize the nuclear structure and function through its interactions with transcription and replication machineries 25, 26. By binding to the nuclear envelope proteins, such as Man1 and nesprins, the nuclear lamina also mediates the connection between the nucleus and the cytoplasmic membrane systems as well as the cytoskeleton 27. Although the nuclear envelope and lamina undergo disassembly in mitosis, it is possible that many components of the disassembled nucleus become organized into the mitotic spindle matrix to facilitate the organization of the membrane system and nuclear content for cell division.

Interestingly, in lower eukaryotes that undergo ‘closed’ mitosis with the spindle assembles inside the intact nuclear envelope, dynein is required for nuclear movement and mitotic spindle and or nucleus orientation, but not for spindle assembly per se 28, 29. The lack of an obvious requirement for dynein in ‘closed’ mitosis could be because that the intact mitotic nucleus functions as the spindle matrix to organize both the nuclear and cytoplasmic contents for division (Fig. S10). Our studies suggest that one important function of dynein and Nudel in animal cell mitosis where the nuclear envelope breaks down (‘open’ mitosis) is to help organize a membranous lamin B matrix that resembles the nuclear envelope and lamina.

Supplementary Material

Refer to Web version on PubMed Central for supplementary material.

Acknowledgements

We thank Dr. Reimer Stick for LB3 monoclonal antibody, Dr. Robert Goldman for the full length LB3 construct, Ms. Shufang He and Ms. Xiaoyan Wang for help with the Biacore experiments, Mr. Dan Ducat and Mr. Ben Goodman for help with egg extracts, Ms. Ona Martin for technical support, Dr. Max Guo and the members of Zheng lab for critical comments. Supported by NIH (GM56312, YZ; MH067880 and P41 RR011823, JRY), Chinese Academy of Sciences (CXTD-S2005-3, XZ), Ministry of Science and Technology of China (2007CB914501, XZ), National Science Foundation of China (30721065 and 30830060, XZ), CFFT computational fellowship (BALCH05X5, BL). YZ is an investigator of Howard Hughes Medical Institute.

References

1. Wynshaw-Boris A. Lissencephaly and LIS1: insights into the molecular mechanisms of neuronal migration and development. Clin Genet. 2007; 72:296–304. [PubMed: 17850624]
2. Nguyen MD, et al. A Nudel-dependent mechanism of neurofilament assembly regulates the integrity of CNS neurons. Nat Cell Biol. 2004; 6:595–608. [PubMed: 15208636]
3. Liang Y, et al. Nudel functions in membrane trafficking mainly though association with Lis1 and cytoplasmic dynein. J Cell Biol. 2004; 164:557–566. [PubMed: 14970193]
4. Liang Y, et al. Nudel modulates kinetochore association and function of cytoplasmic dynein in M phase. Mol Biol Cell. 2007; 18:2656–2666. [PubMed: 17494871]
5. Stehman SA, chen Y, McKenney RJ, Vallee RB. NudE and NudEL are required for mitotic progression and are involved in dynein recruitment to kinetochores. J Cell Biol. 2007; 178:583–594. [PubMed: 17682047]
6. Gruenbaum Y, Margalit A, Goldman RD, Shumaker DK, Wilson KL. The nuclear lamina comes of age. Nat Rev Mol Cell Biol. 2005; 6:21–31. [PubMed: 15688064]
7. Liu J, et al. Essential roles for Caenorhabditis elegans lamin gene in nuclear organization, cell cycle progression, and spatial organization of nuclear pore complexes. Mol Biol Cell. 2000; 11:3937–3947. [PubMed: 11071918]
8. Tsai M-Y, et al. A mitotic lamin B matrix induced by RanGTP required for spindle assembly. Science. 2006; 311:1887–1893. [PubMed: 16543417]
9. Zheng Y, Tsai M-Y. The mitotic spindle matrix, a fibro-membranous lamin connection. Cell Cycle. 2006; 5:2345–2347. [PubMed: 17102624]
10. Helfand BT, Mikami A, Vallee RB, Goldman RD. A requirement for cytoplasmic dynein and dynactin in intermediate filament network assembly and organization. J Cell Biol. 2002; 157:795–806. [PubMed: 12034772]
11. Salina D, et al. Cytoplasmic dynein as a facilitator of nuclear envelope breakdown. Cell. 2002; 108:97–107. [PubMed: 11792324]
12. Beaudouin J, Gerlich D, Daigle N, Eils R, Ellenberg J. Nuclear envelope breakdown proceeds by microtubule-induced tearing of the lamina. Cell. 2002; 108:83–96. [PubMed: 11792323]
13. Lourim D, Kempf A, Krohne G. Characterization and quantitation of three B-type lamins in *Xenopus* oocytes and eggs: increase of lamin L1 protein synthesis during meiotic maturation. J Cell Sci. 1996; 109:1775–1785. [PubMed: 8832400]
14. Herrmann H, Bar H, Kreplak L, Strelkov SV, Aebi U. Intermediate filaments: from cell architechture to nanomechaniscs. Nat Rev Mol Cell Biol. 2007; 8:562–573. [PubMed: 17551517]
15. Tsai M-Y, Zheng Y. Aurora A kinase-coated beads function as microtubule organizing centers and enhance RanGTP-induced spindle assembly. Curr Biol. 2005; 15:2156–2163. [PubMed: 16332542]
16. Vergnolle MA, Taylor SS. Cenp-F links kinetochores to Ndel1/Nde1/Lis1/dynein microtubule motor compolexes. Curr Biol. 2007; 17:1173–1179. [PubMed: 17600710]

17. Feng Y, Walsh CA. Mitotic spindle regulation by Nde1 controls cerebral cortical size. Neuron. 2004; 44:279–293. [PubMed: 15473967]
18. Merdes A, Ramyar K, Vechio J, Cleveland D. A complex of NuMA and cytoplasmic dynein is essential for mitotic spindle assembly. Cell. 1996; 87:447–458. [PubMed: 8898198]
19. Mayer TU, et al. Small molecule inhibitor of mitotic spindle bipolarity identified in a phenotype-based screen. Science. 1999; 286:971–974. [PubMed: 10542155]
20. Merdes A, Cleveland DW. Pathway of spindle pole formation: different mechanisms; conserved components. J Cell Biol. 1997; 138:953–956. [PubMed: 9281574]
21. Merdes A, Heald R, Samejima K, Earnshaw W, Cleveland D. Formation of spindle poles by dynein/dynactin-dependent transport of NuMA. J Cell Biol. 2000; 149:851–862. [PubMed: 10811826]
22. Cao K, Nakajima R, Meyer HH, Zheng Y. The AAA-ATPase Cdc48/p97 regulates spindle disassembly at the end of mitosis. Cell. 2003; 115:355–367. [PubMed: 14636562]
23. Cao K, Zheng Y. The Cdc48/p97-Ufd1-Npl4 complex: its potential role in coordinating cellular morphogenesis during M-G1 transition. Cell Cycle. 2004; 3:422–424. [PubMed: 15004522]
24. Vong QP, Cao K, li HY, Iglesias PA, Zheng Y. Chromosome alignment and segregation regulated by ubiquitination of Surivin. Science. 2005; 310:1499–1504. [PubMed: 16322459]
25. Spann TP, Goldman AE, Wang C, Huang S, Goldman RD. Alteration of nuclear lamin organization inhibits RNA polymerase II-dependent transcription. J Cell Biol. 2002; 156:603–608. [PubMed: 11854306]
26. Spann TP, Moir RD, Goldman AE, Stick R, Goldman RD. Disruption of nuclear lamin organization alters the distribution of replication factors and inhibits DNA synthesis. J Cell Biol. 1997; 136:1201–1212. [PubMed: 9087437]
27. Goldman DG, Yosef G, Moir RD, Shumaker DK, Spann TP. Nuclear lamins: building blocks of nuclear architecture. Genes & Dev. 2002; 16:533–547. [PubMed: 11877373]
28. Xiang X, Fischer R. Nuclear migration and positioning in filamentus fungi. Fungal Genet Biol. 2004; 41:411–419. [PubMed: 14998524]
29. Yamamoto A, Hiroaka Y. Cytoplasmic dynein in fungi: insights from nuclear migration. J Cell Sci. 2003; 116:4501–4512. [PubMed: 14576344]

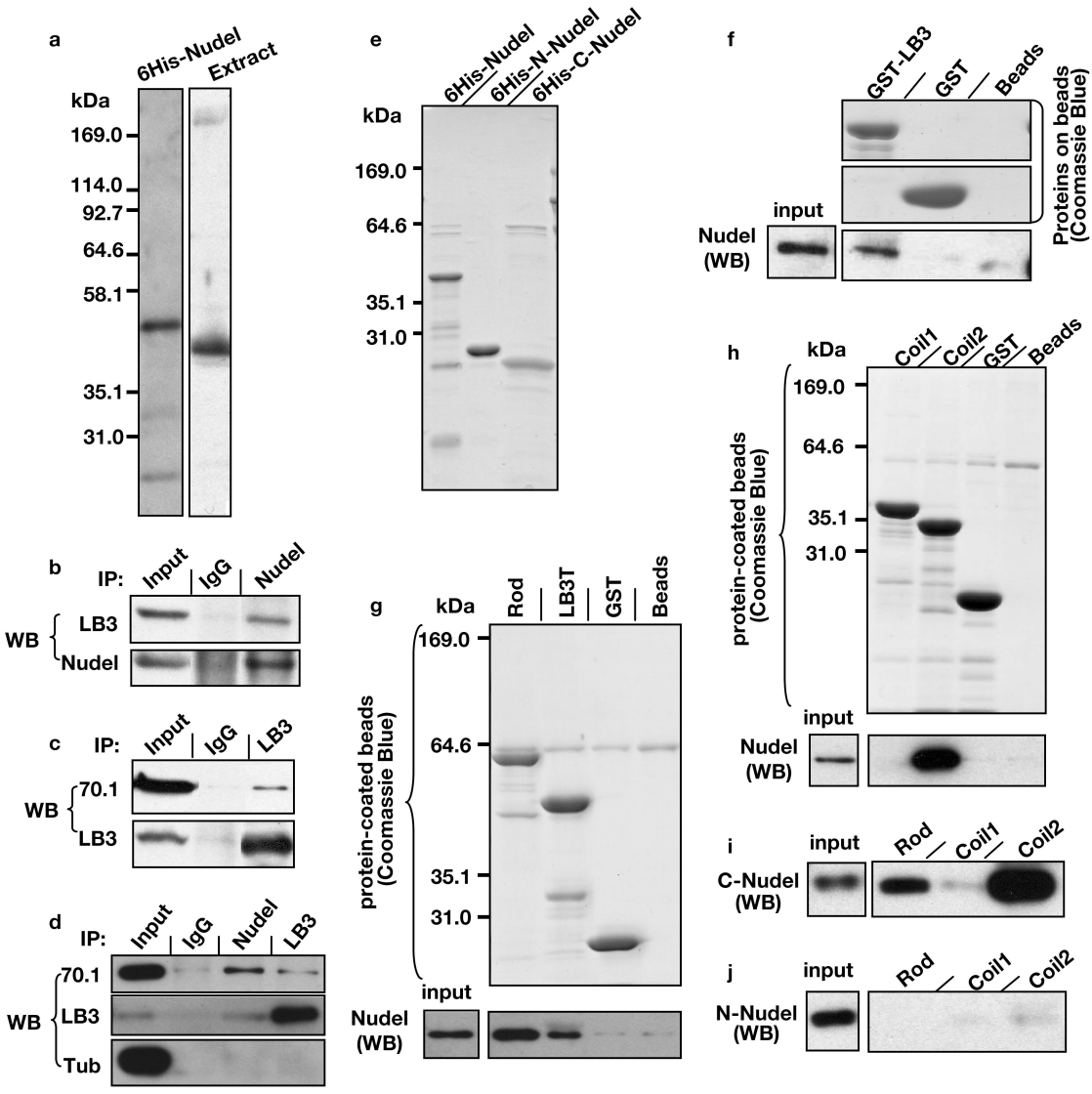

Figure 1.

Interaction of Nudel and dynein with LB3. (**a**) Nudel antibodies specifically recognized purified full length 6His-Nudel and Nudel in *Xenopus* egg extracts by Western blotting. (**b**) Antibodies to Nudel immunoprecipitated (IP) LB3 in egg extracts as judged by Western blotting (WB) analysis. (**c**) Antibodies to LB3 immunoprecipitated dynein, as detected by 70.1 antibody, in egg extracts. **(d)** Antibodies to LB3 or Nudel did not pull-down tubulin from the egg extracts. Immunoprecipitations were carried out in the presence of nocodazole to depolymerize MTs. Equivalent of 0.1 and 10 μl of extracts were loaded for input and for immunoprecipitations, respectively, except for the lanes that show LB3 pull-down LB3 itself where only the equivalent of 0.2 μl of egg extract was loaded. (**e**) Bacterially expressed and purified 6His-tagged full length, N-, or C-terminus of Nudel were analyzed by SDS-PAGE followed by Coommasie blue staining. (**f**) Beads coupled with purified GST-full length LB3 pulled down purified 6His-Nudel. GST-coupled beads or empty beads served as controls. Comparable amount of GST and GST-LB3 were loaded on the beads as judged by

Coomassie Blue staining. 0.033% of the input Nudel and 33% of the precipitate were used for Western blotting (WB). (**g**) Beads coupled with purified GST-LB3-Rod pulled down more 6His-Nudel than beads coupled with GST-LB3T. GST-bound beads or empty beads served as controls. 0.016% of the input Nudel and 16% of the precipitate were loaded for Western blotting. (**h**) Beads coupled with purified GST-LB3-coil2, but not GST-LB3-coil1, pulled down 6His-Nudel. 0.033% of the input Nudel and 16% of the precipitate were loaded for Western blotting. (**i**) Beads coupled with either purified GST-LB3-Rod or purified GST-LB3-coil2, but not GST-LB3-coil1, pulled down purified 6His-C-Nudel. (**j**) Beads coupled with purified GST-LB3-Rod, GST-LB3-coil1, or GST-LB3-coil2 all failed to pull down 6His-N-Nudel. In both (**i**) and (**j**), 0.041% of the input Nudel and 33% of the precipitate were loaded for Western blotting.

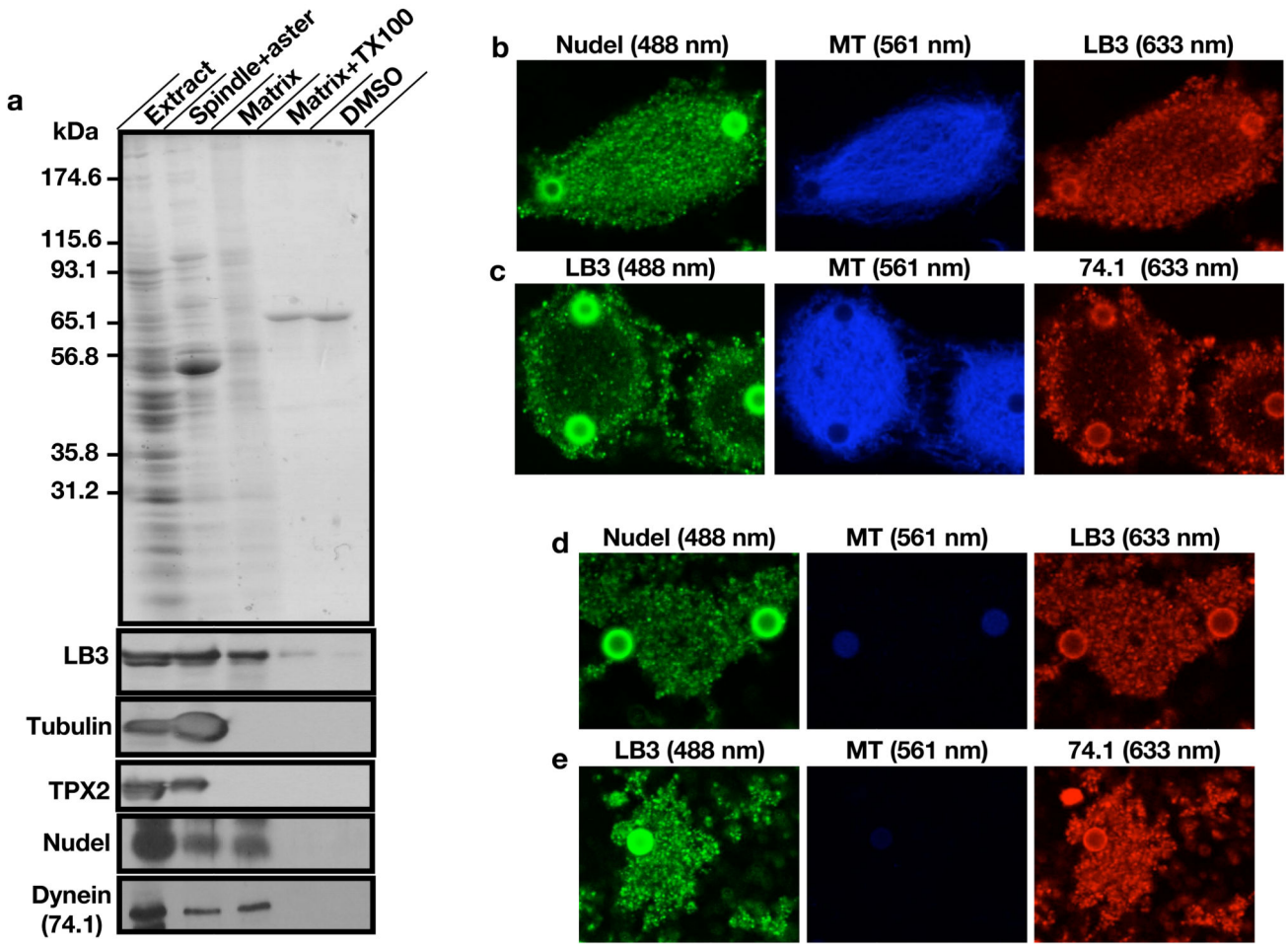

Figure 2.

Identification of Nudel and dynein in the lamin B spindle matrix. (**a**) Isolation and characterization of the mitotic spindle matrix. AurA-beads were used to stimulate MT assembly in the presence of RanGTP. MT structures (Spindle+aster) were retrieved using a magnet. After depolymerizing MTs using nocodazole and XB buffer washes, the matrix associated with beads in RanGTP reactions was either directly analyzed on SDS-PAGE (Matrix), or treated with 0.5% Triton X100 (Matrix+TX100) and analyzed. Matrix failed to assemble when MT assembly was stimulated by DMSO and then depolymerized (DMSO). Western blotting analyses showed that the isolated matrix retained lamin B3 (LB3), Nudel, and dynein. In contrast, vast majority of TPX2, and tubulin were removed from the matrix after MT depolymerization. (**b**) Localization of Nudel and LB3 on spindles. Nudel and LB3 were detected using rabbit anti-Nudel and mouse anti-LB3 antibodies, respectively. (**c**) Localization of dynein and LB3 on spindles. Dynein and LB3 were detected using the mouse monoclonal antibody 74.1 (detecting the dynein intermediate chain) and the rabbit anti-LB3 antibody, respectively. (**d** and **e**) Localization of Nudel, LB3, and dynein on the spindle matrix. Images were acquired using a confocal microscope (Leica SP5). Rhodamine tubulin was used to detect MTs in **b–e** and numbers in parentheses indicate laser lines used. Scale, magnetic beads (2.8 μm in diameter).

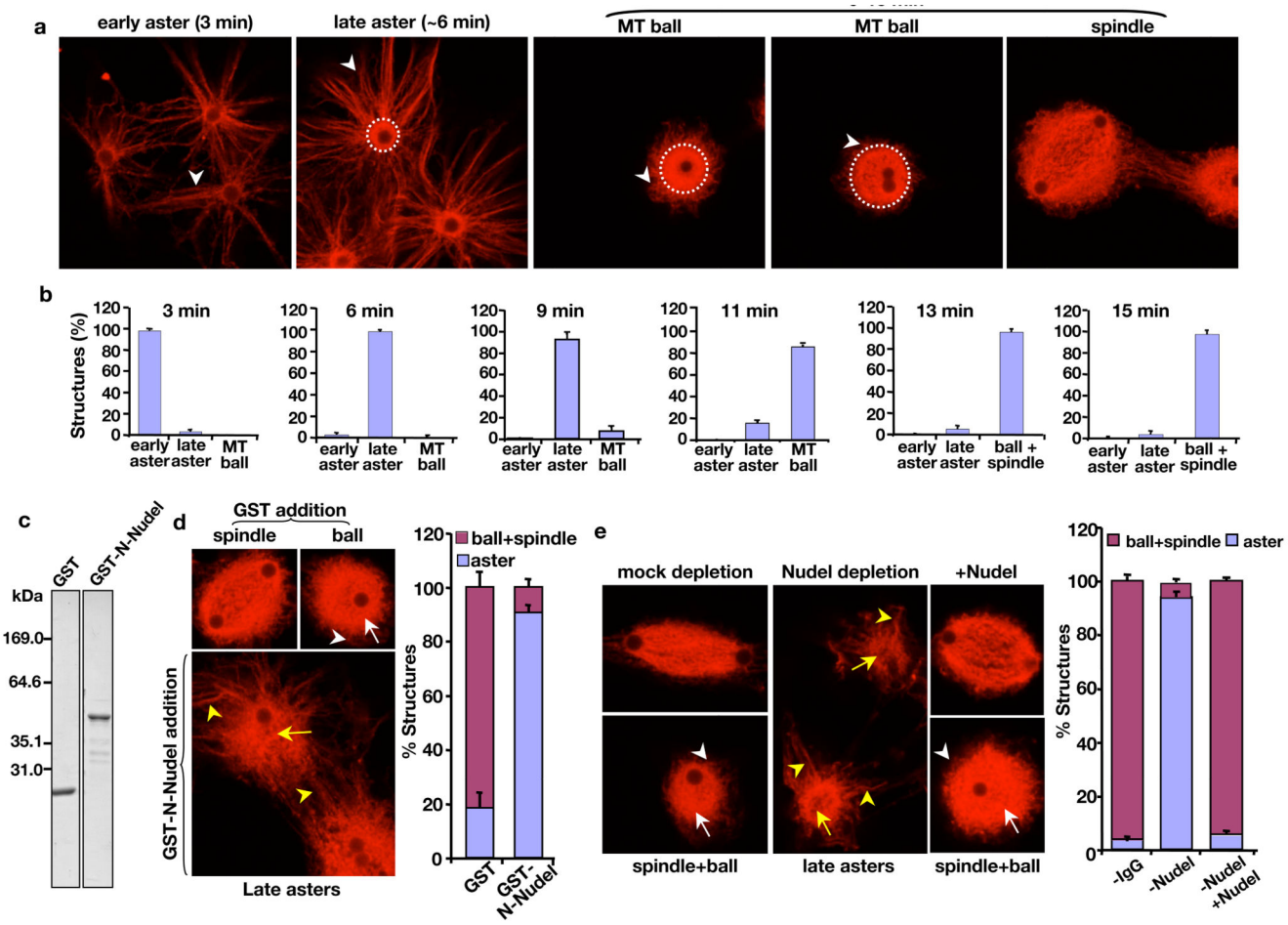

Figure 3.

Effect of Nudel on MT organization during spindle assembly induced by AurA-beads and RanGTP. (**a** and **b**) Progression of spindle morphogenesis induced by AurA-beads. (**a**) Early asters formed in the first 1'–3' had astral MTs (white arrowhead) attached to the bead surface. Late asters formed at ~6' had an increasing density of MT astral arrays (white arrowhead) attached to a clear bright MT core (outlined by a white dashed circle). MT balls, which appeared after 9', had an expanding bright MT core (outlined by white dashed circles) surrounding the beads and with time the astral MT arrays (white arrowheads) became fewer and shorter than those seen in early and late asters. Most structures were MT balls and spindles at 13'–15'. (**b**) Quantification of different MT structures at the indicated time point. (**c**) Bacterially-expressed and purified GST or GST-tagged N-terminal half (amino acids 1–201) of Nudel was analyzed by SDS-PAGE followed by Coomassie blue staining. (**d**) Effects of excess purified GST-N-Nudel on MT morphogenesis during spindle assembly induced by AurA-beads. GST-N-Nudel or GST was added at ~50-fold molar excess of endogenous Nudel (50–100 nM). Whereas MT balls formed in the presence of GST had dense MT cores (white arrow) associated with a thin and short array of MTs (white arrowhead), asters formed in the presence of GST-N-Nudel had long MT arrays (yellow arrowheads) attached to a MT core that was not as densely packed with MTs as the controls (compare the structures pointed to by white and yellow arrows). (**e**) Effects of Nudel

depletion on MT morphogenesis during spindle assembly induced by AurA-beads. Depletion of Nudel from *Xenopus* egg extracts resulted in a severe block of MT ball and spindle assembly, which were rescued by addition of purified 6His-Nudel. Examples of spindles, MT balls, and MT asters are shown. White arrows and arrowheads point to the dense MT core and short MT arrays, respectively, of MT balls found in mock depleted or Nudel depleted and rescued extracts. Yellow arrows and arrowheads point to the less densely packed MT core and long MT arrays, respectively, of MT asters found in Nudel-depleted egg extracts. Rhodamine-labeled tubulin was used for MT visualization. Images were acquired using a confocal microscope (Leica SP5). Scale, magnetic beads (2.8 μm in diameter). Error bars, standard deviation from >3 independent experiments.

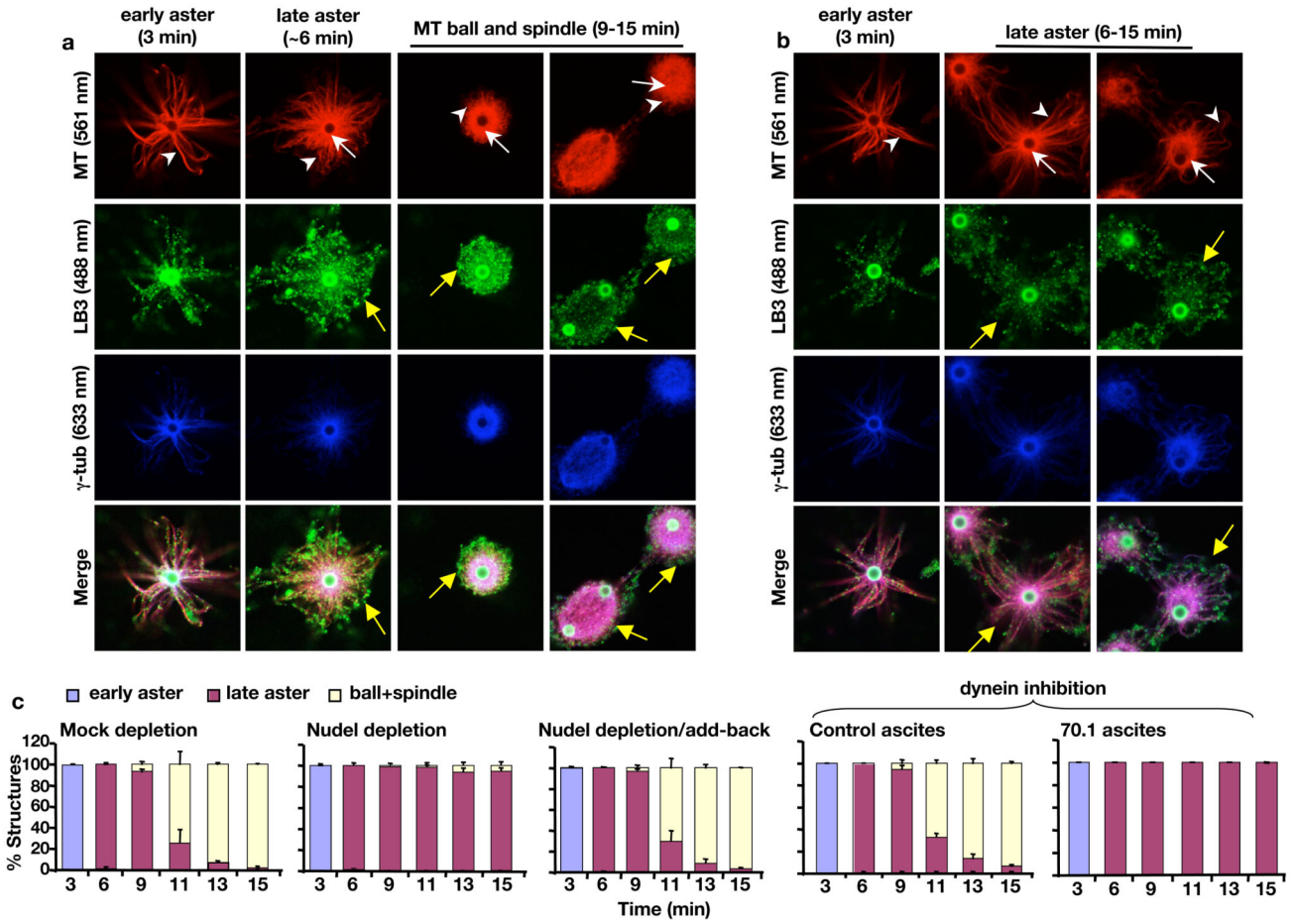

Figure 4.

Effects of disrupting Nudel or dynein on spindle assembly and LB3 localization in the AurA-bead based assay. (**a**) Progression of spindle morphogenesis and LB3 assembly in mock-depleted egg extracts. LB3 was found along MTs of early asters. As early asters transformed into late aster (white arrows and arrowheads point to bright MT cores and astral MTs, respectively), meshworks of LB3 were seen to surround the late asters. High levels of LB3 were also found throughout the MT balls and spindles. The bright green staining of the beads was caused by the rabbit secondary antibody that recognized anti-AurA antibodies coated on the beads. Yellow arrows point to the LB3 network surrounding the late aster, MT ball, and spindle. (**b**) Progression of MT and LB3 assembly in Nudel-depleted egg extracts. Formation of early and later asters and the accumulation of γ-tubulin on the AurA-beads occurred normally. However, there was a lack of MT ball and spindle assembly in the absence of Nudel. White arrows and arrowheads point to MT cores and astral MTs, respectively. There was a diminished LB3 network surrounding the late asters as compared to the late aster in the control (compare yellow arrows in the late asters in a and b). (**c**) Quantification of MT structures at different time points and treatment conditions. All images were acquired on a Leica SP5 confocal microscope with laser lines used indicated in parentheses. Scale, magnetic beads (2.8 μm in diameter). Error bars, standard deviation from >3 independent experiments.

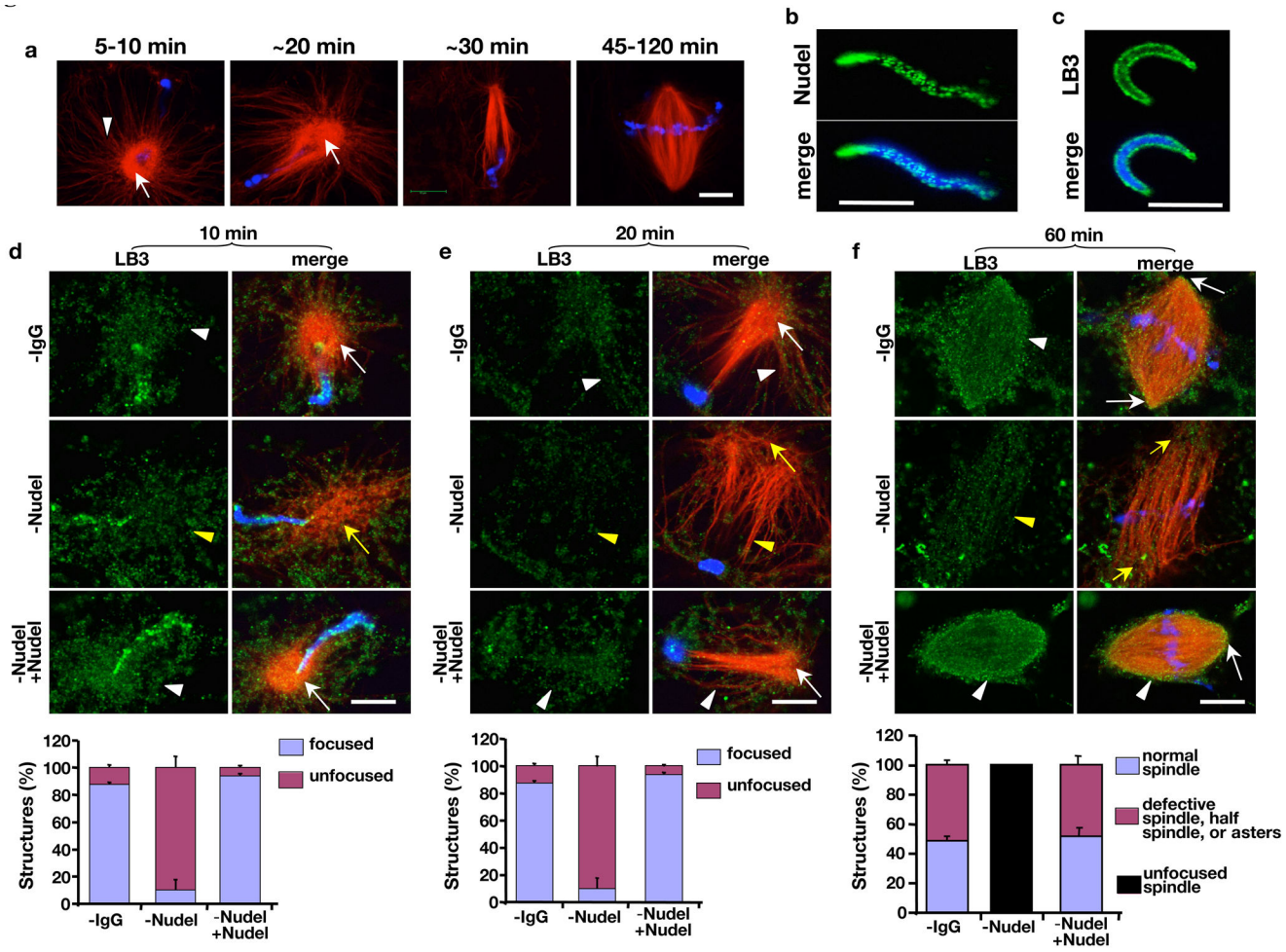

Figure 5.

Requirement of Nudel in MT organization and LB3 assembly during spindle morphogenesis induced by sperm. (**a**) Time course of spindle assembly induced by sperm chromatin. Sperm asters assembled in the first 5'–10' had bright MT cores (white arrow) attached to long astral MT arrays (white arrowhead). The astral arrays underwent polarization toward sperm chromatin to form half spindles in 20–30', which further organizing into bipolar spindles between 45–120'. (**b** and **c**) Localization of Nudel (**b**) and LB3 (**c**) on the demembranated sperm. (**d–f**) Effects of Nudel depletion on MT organization and LB3 accumulation during spindle assembly. Shown are MT, LB3, and sperm chromatin at 10' (**d**), 20' (**e**), and 60' (**f**). Nudel depletion caused disorganization of MT asters (**d**), polarized MT structures (**e**), and spindle poles (**f**) (compare yellow and white arrows). Although LB3 was found throughout the disorganized asters formed in the first 10' in the absence of Nudel (compare white and yellow arrowheads in **d**), there was a clear reduction of LB3 on MTs by 20' (**e**) and 60' (**f**) as compared to those in mock-depleted or Nudel-rescued egg extracts (compare yellow and white arrowheads in **e** and **f**). MT structures were quantified in the graphs below the images. DAPI (blue) stained the sperm DNA. All images were acquired on a Leica SP5 confocal microscope. Scale bar, 10 μm. Error bars, standard deviation from >3 independent experiments.

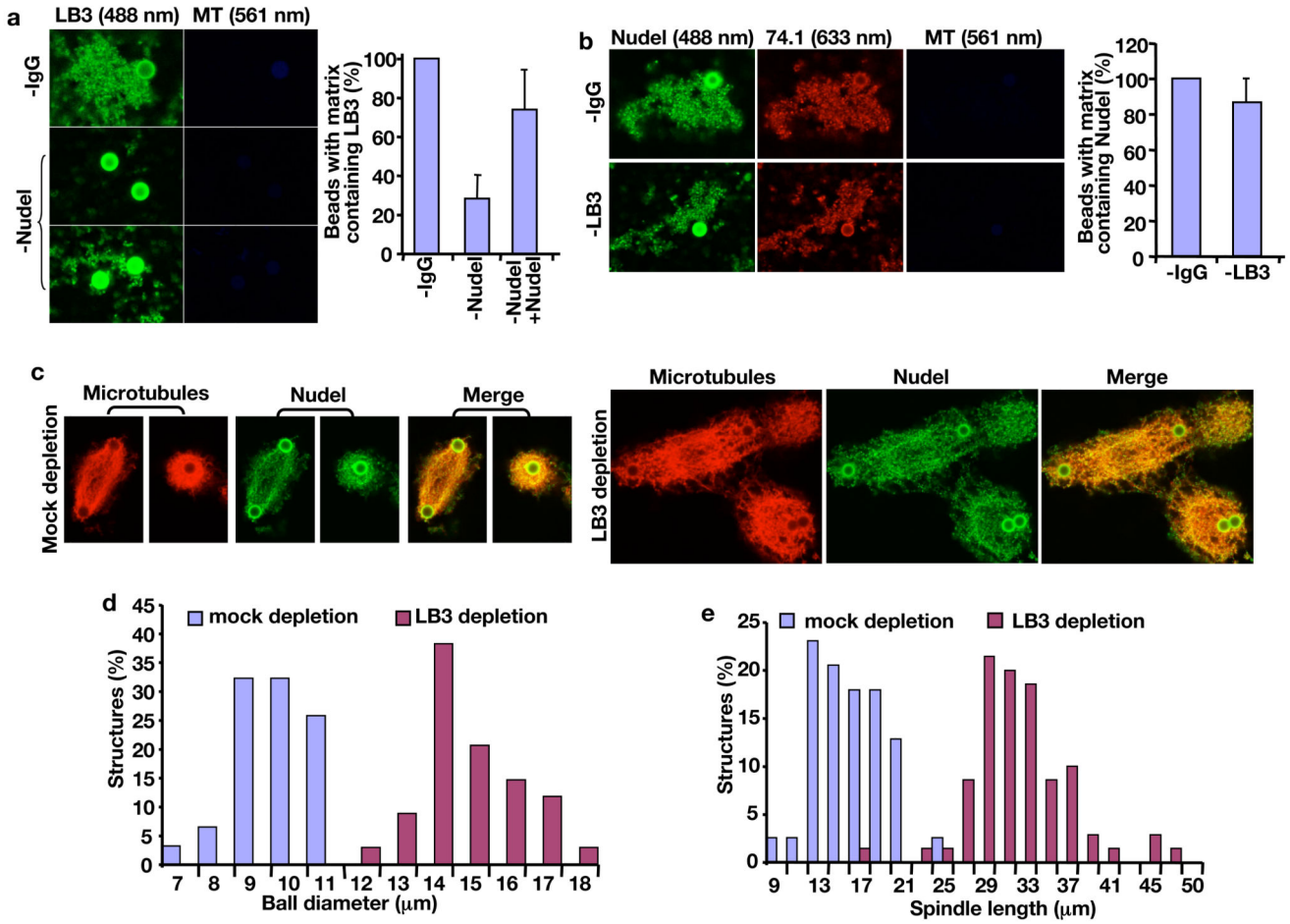

Figure 6.

Nudel promotes assembly of the spindle matrix and MT organization. (**a**) Effects of Nudel depletion on assembly of LB3-containing matrices. In the absence of Nudel, most beads were not associated with LB3-containing matrices, while only a few beads were associated with LB3-containing matrices that were smaller in size compared to controls. Addition of purified 6His-Nudel rescued formation of LB3 matrices (quantifications on the right were carried out blindly). (**b**) Effects of LB3 depletion on formation of matrices containing Nudel and dynein. Depletion of LB3 still allowed the formation of Nudel and dynein-containing matrices (quantifications on the right were carried out blindly). (**c**) Effects of LB3 depletion on MT structures induced by AurA-beads. Shown are representative spindles and MT balls formed in mock- and LB3-depleted egg extracts. Rhodamine tubulin and Nudel antibodies were used to visualize MT structures. (**d** and **e**) Quantification of the diameter of MT balls and the length of spindles at 15’ of reactions. 40–150 structures assembled were measured in each category. All images were acquired on a Leica SP5 confocal microscope with laser lines used indicated in parentheses. Scale, magnetic beads (2.8 μm in diameter). Error bars, standard deviation from >3 independent experiments.

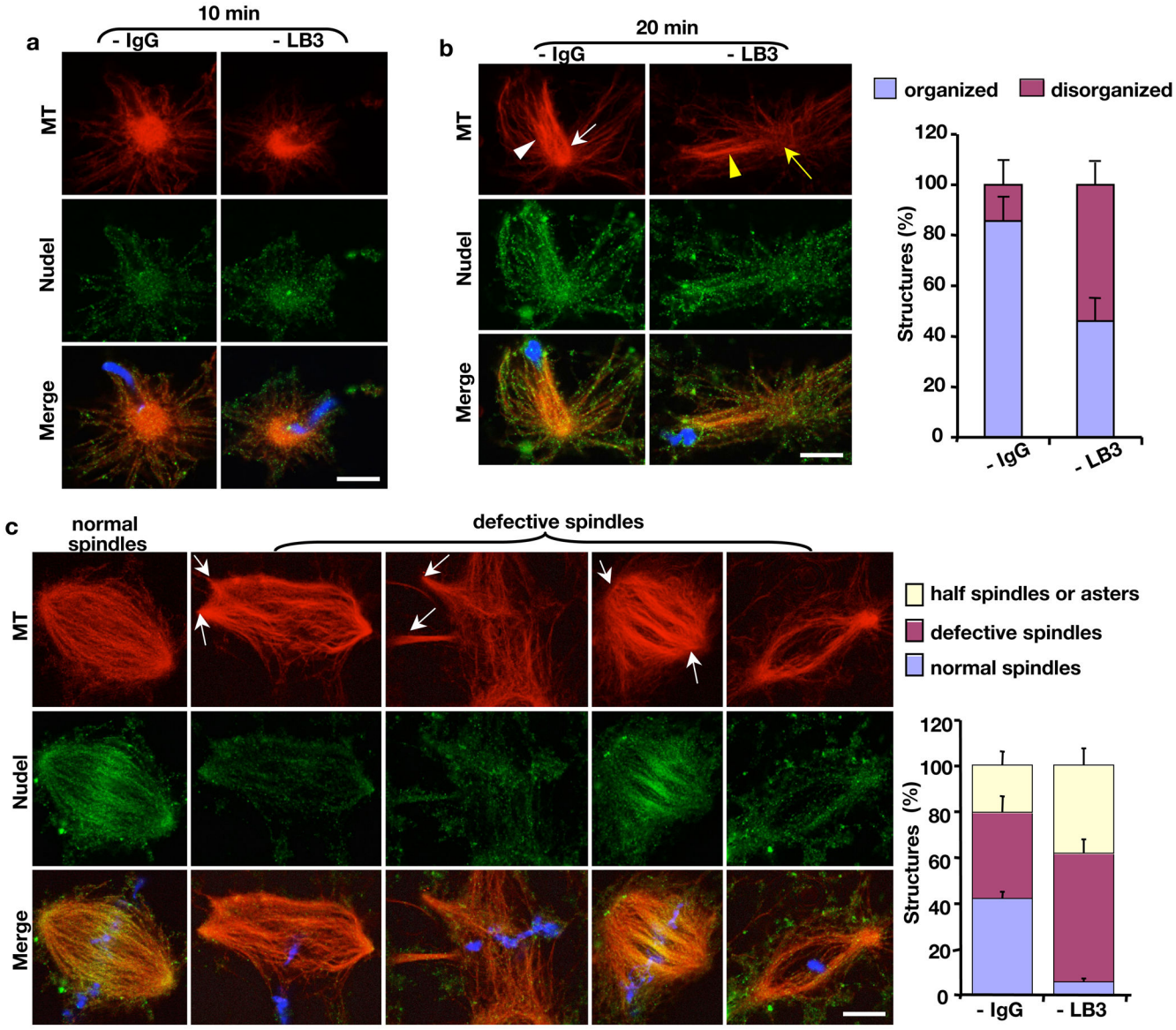

Figure 7.

Effects of LB3 depletion on MT structures induced by sperm chromatin. (**a**) Assembly of MT asters in the first 15' was not affected by LB3 depletion. (**b**) Depletion of LB3 disrupted the organization of polarized MT arrays toward the sperm chromatin after 15' (compare white and yellow arrows and arrowheads). (**c**) Depletion of LB3 resulted in spindle defects at 45'–120', including multipolar spindles, spindles with splayed poles, and spindles with few MTs. White arrows point to the defective spindle poles. DAPI (blue) stained the sperm DNA. All quantifications were carried out blindly. All images were acquired on a Leica SP5 confocal microscope. Scale bars, 10 μm. Error bars, standard deviation from >3 independent experiments.